

Application of Nilsson model for deformed nucleus in relativistic heavy ion collisions

S. K. Tripathy^{1,2}, M. Younus^{3,*}, P. K. Sahu¹, and Z. Naik²

¹Institute of Physics, HBNI, Sachivalaya Marg, Bhubaneswar 751005, India

²Sambalpur University, Jyoti Vihar, Burla, Sambalpur, Odisha 768019, India

³Nelson Mandela University, Port Elizabeth, 6031, South Africa

June 11, 2018

Abstract

Electron scattering methods, involving nucleus which have little or no intrinsic deformation suggest nucleon distribution to be of Fermi type. This distribution is further parameterised as Wood Saxon (WS) distribution, where an uniform charge density with smoothed-out surface have been implemented. Incorporating shape modification in WS, earlier attempts were made to explain observables in deformed nuclear collisions, such as charged particle multiplicity. In this work, we use an alternate approach known as Nilsson model or Modified Harmonic Oscillator (MHO), to explain charged particle multiplicity in U+U collisions at top RHIC energy. We have implemented the formalism in HIJING model and we found that the model describes the experimental data to an extent.

Keywords : Monte Carlo simulations, deformed nuclei, Charged particle production

PACS: 21.60.Ka, 25.75.Dw

1 Introduction

One of the goals of heavy ion collisions is to produce a system of de-confined quarks and gluons (known as QGP) at high temperatures and densities. Existing experimental data and theoretical simulations indicate the formation of collective phenomena at the early stage of QGP. Some of the experimental observable suggests that initial anisotropy in partons' configuration affects the final state particle and hence, corresponding observables. It is known that both kinematics and dynamics of heavy ion collisions depend upon collision centrality as well as nucleon distributions of colliding nuclei. The multi-scattering of the participant nucleons and their constituent partons give rise to some novel phenomena such as nuclear shadowing, Cronin effects etc [1, 2]. Similarly, non-participating nucleons or spectators contribute to the chiral magnet effects produced in QGP. So, in order to simulate and study QGP dynamics, initial state geometry plays a very important role and must be precisely evaluated and determined.

In case of heavy (little or zero intrinsic deformed) spherical nuclei (approx. Au, Pb etc) collisions, the standard Wood-Saxon(WS) distribution [3] of nucleons inside a nucleus gives us charged particle multiplicity distributions (N_{ch}). However for collisions of U nuclei, owing to their prolate shape, they can undergo collisions with body-body, tip-tip, or body-tip or with any random configuration and may provide different pre-equilibrium conditions than that described

*younus.presi@gmail.com

by WS for spherical nuclei collisions. Therefore, Modified Wood-Saxon(MWS) [4] distribution is applied to U+U collision system in order to explain experimental data [5, 6, 7, 8, 9, 10]. Many in-depth and first-hand information on deformed system could be obtained from these studies using MWS.

In this paper, we have taken an alternative approach for calculating N_{ch} distribution. We have started from Nilsson potential or Modified harmonic oscillator(MHO) potential [11, 12], to derive and develop the MHO nucleon distribution for Uranium nucleus and calculate charged particle multiplicity distribution using Glauber formalism within HIJING model [13].

The paper is organised as follow. In Sec 2 we will present derivation of Nilsson formalism and will explain in detail analytical form of various terms associated with it. In Sec 3 we will show results from this formalism along with Wood Saxon We will compare our results along with published data in this section as well. Finally we will summarise in Sec 4.

2 Nilsson distribution/Modified harmonic oscillator(MHO)

Using semi-classical partition function [16]

$$Z_{sc}(\beta) = \frac{2}{\hbar^3} \int e^{-\beta H_{sc}} d^3r d^3p, \quad (1)$$

one may derive the the standard Thomas-Fermi relations (Leading Order) for nucleons' single particle distribution $\varrho(r)$, and energy densities inside a nucleus for a given potential $V(r)$ in the Hamiltonian, $H_{sc} = \frac{1}{2} \sum m_i r_i^2 + V(r) + f(r, p)$ as,

$$\varrho(r) = \frac{1}{3\pi^2} \left[\frac{2m}{\hbar^2} (\lambda_0 - V(r)) \right]^{3/2} \frac{m^*(r)}{m} \quad (2)$$

Here $f(r, p)$ contains interaction terms such as orbital angular momentum, l etc., ($V_l = -\kappa\mu\hbar\omega_0(l^2 - \langle l^2 \rangle)$). The higher order corrections in orders and terms of \hbar have been calculated [17]. Here as a first attempt, we have derived and used the leading order term as shown in [18]. Here, $V(r, \theta)$ is the Nilsson potential, λ_0 is the cut on turning point for Nilsson potential, when $\lambda_0 - V(r)$ becomes negative. $m^*(r)$ is the effective mass and can be written as:

$$m^*(r) = m/(1 - 2v_l m r^2) \quad (3)$$

Where $v_l = \kappa\mu\omega_0/\hbar$, k and μ are parameters.

Binomial expansion of Eq. 2 can be written as follows:

$$\begin{aligned} \varrho(r) &= \frac{1}{3\pi^2} \left(\frac{2m}{\hbar^2} \right)^{3/2} \lambda_0^{3/2} [1 - V(r, \theta)/\lambda_0]^{3/2} \frac{m^*(r)}{m} \\ &= \frac{1}{3\pi^2} \left(\frac{2m}{\hbar^2} \right)^{3/2} \lambda_0^{3/2} [1 - (3/2)V(r, \theta)/\lambda_0 \\ &\quad + (3/8)(V(r, \theta)/\lambda_0)^2 - (3/48)(V(r, \theta)/\lambda_0)^3 \\ &\quad + \mathcal{O}((V(r)/\lambda_0)^4)] \frac{m^*(r)}{m} [1/fm^3] \end{aligned} \quad (4)$$

Eq. 4 is in expanded form assuming $\lambda_0 > V(r, \theta)$. Also, the value assumed for $\lambda_0 \gtrsim V(R_\theta, \theta)$, as $\varrho(r)$ goes smoothly to zero.

We have taken the surface radius of the uranium nucleus as [19]

$$\begin{aligned} R|_{\theta=0} &= R_A \left(1 - \frac{2\epsilon_2}{3} \right) [fm], \\ R|_{\theta=\pi/2} &= R_A \left(1 + \frac{\epsilon_2}{3} \right) [fm] \end{aligned} \quad (5)$$

where, $R_A(= 1.2A^{1/3})$ is the surface radius of undistorted uranium nucleus.

The Nilsson form of $V(r, \theta)$ is taken assuming anharmonic oscillator equation for the distorted nucleus (also known as modified harmonic oscillator, MHO) is as follows:

$$V(r, \epsilon, \theta) = \frac{1}{2}\hbar\omega_0(\epsilon)\varrho_t^2 \left[1 + 2\epsilon_1\sqrt{\frac{4\pi}{3}}Y_{10}(\theta_t) - \frac{2}{3}\epsilon_2\sqrt{\frac{4\pi}{5}}Y_{20}(\theta_t) + 2\sum_{\lambda=3}^{\lambda_{max}}\epsilon_\lambda\sqrt{\frac{4\pi}{2\lambda+1}}Y_{\lambda 0}(\theta_t) \right], \quad (6)$$

Considering even order terms up to 2nd order as mentioned in Ref. [18]

$$V(r, \epsilon, \theta) = \frac{1}{2}\hbar\omega_0(\epsilon)\varrho_t^2 \left[1 - \frac{2}{3}\epsilon_2\sqrt{\frac{4\pi}{5}}Y_{20}(\theta_t) \right] [MeV] \quad (7)$$

where the spherical harmonics,

$$Y_{20}(\theta) = \frac{1}{4}\sqrt{\frac{5}{\pi}}(3\cos^2\theta - 1) \quad (8)$$

and

$$\cos\theta_t = \left[\frac{1 - (2/3)\epsilon_2}{1 + \epsilon_2[(1/3) - \cos^2\theta]} \right]^{1/2} \cdot \cos\theta \quad (9)$$

One can also calculate,
 $\omega_0(\epsilon) = \omega_{00} (1 - \frac{1}{3}\epsilon_2^2 - \frac{2}{27}\epsilon_2^3)^{-1/3}$
 where ω_{00} value can be calculated from the expression,
 $\hbar\omega_{00} = 41 \times A^{-1/3}$ MeV (for U, $A = 238$).

The position of the nucleon from nucleus centre, ϱ_t in the stretched spherical coordinates is given by

$$\varrho_t^2 = \xi^2 + \eta^2 + \zeta^2 [fm^2]$$

where $\xi = x[\frac{m\omega_0(\epsilon)}{\hbar}(1 + \frac{1}{3}\epsilon_2)]^{1/2}$, $\eta = y[\frac{m\omega_0(\epsilon)}{\hbar}(1 + \frac{1}{3}\epsilon_2)]^{1/2}$ and $\zeta = z[\frac{m\omega_0(\epsilon)}{\hbar}(1 - \frac{2}{3}\epsilon_2)]^{1/2}$.

Therefore, we have

$$\Rightarrow \varrho_t^2 = r^2 \frac{m\omega_0(\epsilon)}{\hbar} [\sin^2\theta(1 + \frac{1}{3}\epsilon_2) + \cos^2\theta(1 - \frac{2}{3}\epsilon_2)] .$$

We have also used quadrupole deformation parameter in our current work [18]

$$\epsilon_2 = 0.944\beta_2 - 0.122\beta_2^2 + 0.154\beta_2\beta_4 - 0.199\beta_4^2 \quad (10)$$

Value of β_i are mentioned in Table of Ref. [20].

Thus, we have Nilsson single particle distribution for nucleons inside Uranium nucleus from Eq. 4.

Finally, we have implemented Nilsson distribution in the in-built Glauber formalism of HIJING. We have taken top RHIC energy (U+U $\sqrt{s_{NN}}=193$ GeV) and charged particles for our calculations. In HIJING, density distributions generate transverse position of individual nucleons. Between each pair of colliding nucleons, impact parameter is calculated using their transverse positions. Eikonal formalism, which uses straight line trajectories between two nucleons is used to calculate probability of collision.

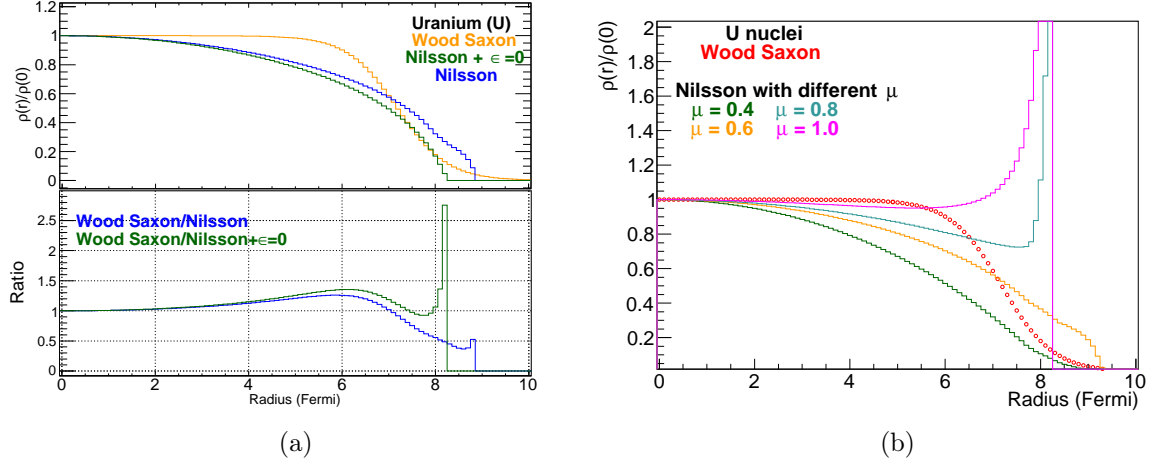


Figure 1: (Color online) In the top plot of Fig 1a density distribution for Wood-Saxon(Orange), Nilsson (Blue) and Nilsson with deformation parameter ($\epsilon = 0$) in (Green) in U nuclei are shown. In the bottom plot, ratio between them are shown. In the Fig 1b It is shown that for one of μ values of Nilsson density distribution, how it converges to Wood Saxon.

3 Results and discussions

We have shown normalised nucleon density in Uranium nucleus using Nilsson(MHO) and standard Wood-Saxon(WS) in Fig. 1a. Here, we see that distribution from MHO drops rapidly and faster than WS. It is in agreement with earlier study by Bengtsson et al., [18] that MHO drops as $\sim e^{-\alpha r^2}$, while WS drop as $\sim e^{-\alpha r}$, asymptotically. From $r = 4$ fm onwards, the ratio of MHO shows a deviation from unity.

Earlier results[14, 15] from electron scattering experiments, suggest a little or zero intrinsic deformations for the nuclei, viz. Ca, V, Co, In, Sb, Au, Bi and C. This investigation also showed that, charge distribution is flat at the central region of the nucleus. Experimental observations however did not include, how the nucleons' distribution would look like for the intrinsic deformed nuclei, such as Hf, Ta, W, U etc. On the theoretical front, we know that MWS successfully retains the flat central region even for the deformed nuclei. Our default results using Nilsson density distribution, shows charge density although remains flat in the most central part, starts deviating from central flat region from 2-3 fms onwards. However, adjusting one of the parameter of Nilsson density (i.e. μ), it goes closer to Wood-Saxon's central flat region even beyond 3 fms as shown in Fig 1b.

To investigate further on our formalism on reproducibility of spherical nuclei, we have plotted minimum bias charged particle multiplicity (N_{ch}) for Au+Au collision at $\sqrt{s_{NN}} = 200$ GeV using WS and MHO (with $\epsilon=0$) in HIJING model in Fig. 2a. WS distribution within HIJING retains the profile shape when compared to experimental results, but gives non-zero charged particle production probability beyond available multiplicity bins from experimental data. On the other hand, MHO with zero deformity reduces the WS estimation in high multiplicity region to some extent, keeping the profile shape almost intact like WS. However, MHO overestimates the experimental data. The plateau region is successfully reproduced by both WS and MHO.

We have plotted our estimation of N_{ch} for U+U collisions at $\sqrt{s_{NN}} = 193$ GeV, with MHO and WS formalism from HIJING in Fig 2b. MHO result is compared to STAR experimental data and keeps the shape intact to an extent, while WS show greater multiplicity than MHO. Here we have shown Nilsson results with random angle orientation of target and projectile nuclei(Nilsson-random), with $\theta = 0$ (Nilsson-tip) and $\theta = \pi/2$ (Nilsson-body). We observe that, random angle average and body-body configuration yields similar results, while tip-tip configuration gives non-zero probability for twice the magnitude of no. of charged particles from random

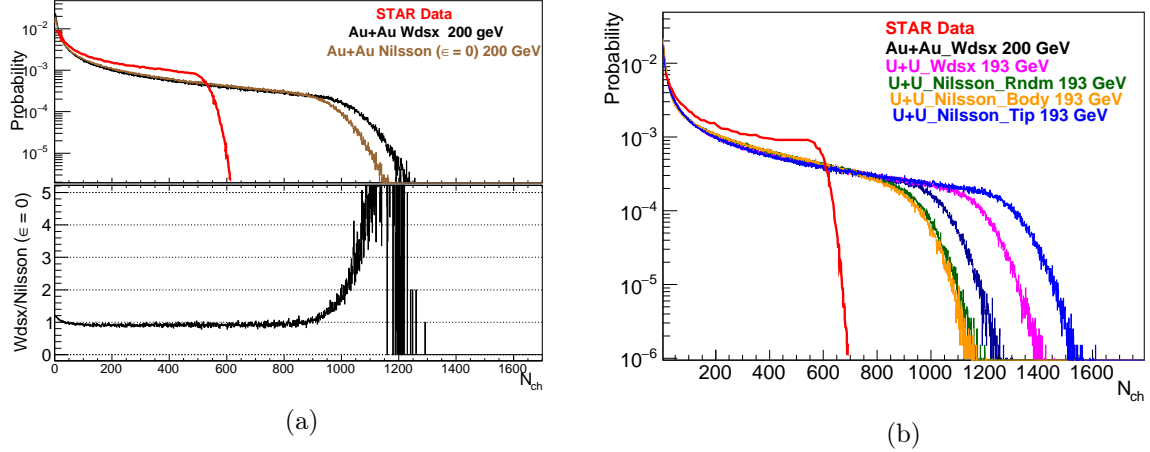


Figure 2: (Color online) In Fig. 2a HIJING N_{ch} distribution using Wood Saxon and Nilsson (with $\epsilon = 0$) for Au+Au 200 GeV in the top panel along with experimental data [21]. Ratio of Wood Saxon to Nilsson are shown in bottom panel. In Fig. 2b HIJING N_{ch} plotted for different configurations of U nuclei along with experimental data [22].

configurations.

We have plotted charged particle pseudo-rapidity distribution ($dN_{ch}/d\eta$) for most central collisions (0 – 5%) in U+U collision at $\sqrt{s_{NN}} = 193$ GeV, with MHO and WS formalisms from HIJING in Fig 3a. MHO gives lower estimates of rapidity distribution compared to WS. In the similar way of Fig 2b, we observe in Fig 3a that, Nilsson with random angle gives consistent result with body-body configuration but tip-tip configuration yields higher magnitude. We have plotted, $dN_{ch}/d\eta$ vs. centrality for U+U collision at $\sqrt{s_{NN}} = 193$ GeV from HIJING with WS and MHO formalism in Fig 3b. We have compared our results with experimental data[23]. Although MHO shows improvement in central collisions regions than WS, our results with MHO for the peripheral collisions divert from WS output.

We present average momentum, $\langle p_T \rangle$, of charged hadrons in Fig. 4. We observe that body and random configurations of colliding uranium nuclei yield particles which show their average momentum independent of centralities of collisions and remain almost flat, while other configurations exhibit a downward moving slope with $\approx 20\%$ deviation from random configurations. We also observe a reverse in the trend between tip-tip to random configuration, when we go from central to peripheral collision.

Transverse momentum spectra of charged hadrons are presented in Fig 5. In the top plot of Fig. 5a, we have shown our results for most central (0-5%, open markers) and most peripheral (60-80%, solid markers) collisions in U+U collision system alongside Au+Au system. In the bottom plot, we have shown the ratios between the various configurations of U+U ($\sqrt{s_{NN}} = 193$ GeV) with Au+Au ($\sqrt{s_{NN}} = 200$ GeV). We observe that, the ratios vary within a broad range of 60% below unity to 50% above. At both centralities, we find ratios from random configurations match with ratios from body-body configurations. For the most central collisions, the ratios of particle yields from Au+Au to U+U tip-tip configurations differ almost by a large factor of 5. The random or body-body yields seem to be always greater than the tip-tip U+U collisions when compared to Au+Au yields. On the other hand, the tip-tip configuration in peripheral collisions shows lesser value than Au+Au with 60% lower yields, while in the case of body-body or random configurations in peripheral collisions, we have ratios showing 2% higher yields than Au+Au. We also observe that irrespective of the centralities, the ratios are independent of particle transverse momentum, p_T . In the Fig 5b, we calculated the similar ratios, but instead of gold nuclei, we have taken uranium nuclei assuming zero deformity. The collisions energy is taken to be $\sqrt{s_{NN}} = 193$ GeV, for all the systems in this case. Here too we find similar trends as

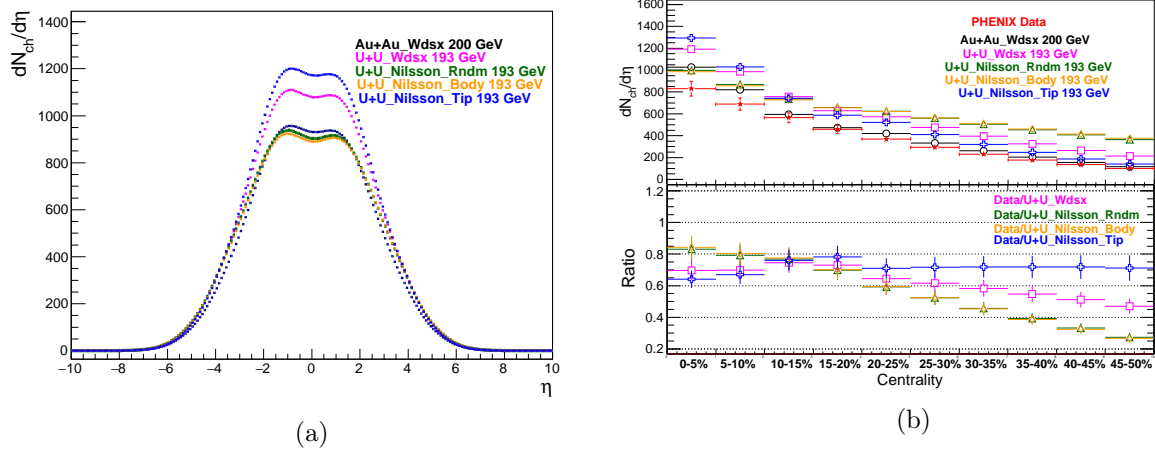


Figure 3: (Color online) HIJING $dN_{ch}/d\eta$ distribution for central collisions (0 – 5%) from WS and MHO (random angle, tip-tip($\theta = 0$) and body-body ($\theta = \pi/2$)) is shown in Fig 3a. $dN_{ch}/d\eta$ with centrality shown in Fig 3b along experimental data [23].

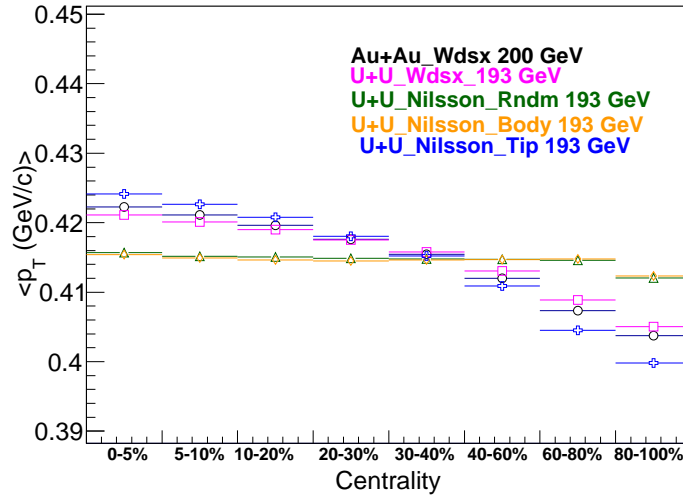


Figure 4: (Color online) $\langle p_T \rangle$ distribution of charged hadron from WS and MHO (random angle, tip-tip($\theta = 0$) and body-body ($\theta = \pi/2$)).

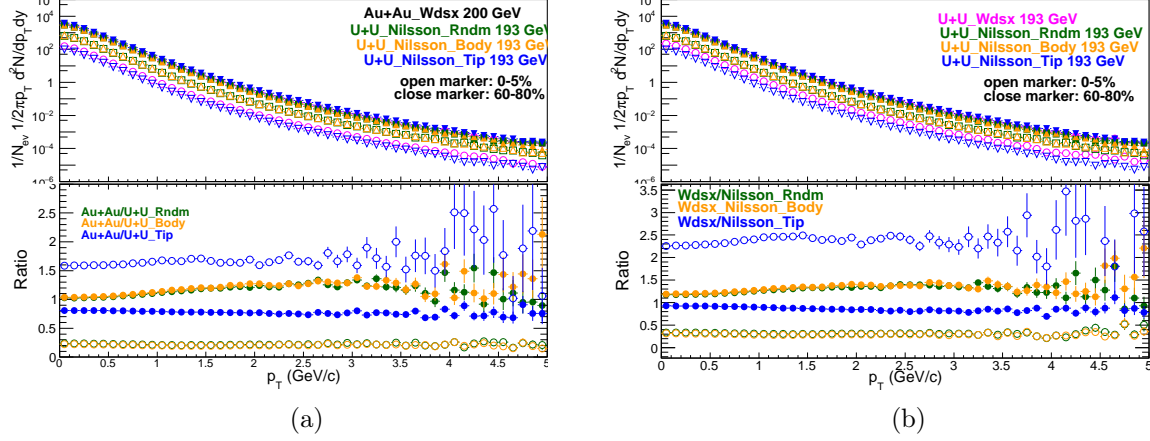


Figure 5: (Color online) p_T spectra of charged hadron in Ws and MHO formalism (with different configurations) in most central and peripheral collision. Results are compared with Au+Au 200 GeV and U+U 193 GeV.

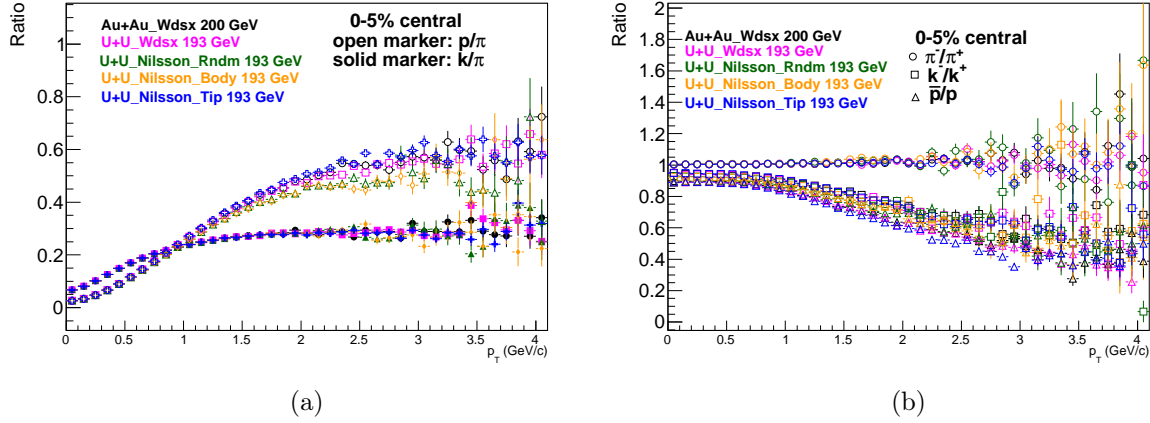


Figure 6: (Color online) particle ratio in most central collision in Ws and MHO formalism (with different configurations).

in previous plot but the variations in the ratios have doubled for central collisions as compared to ratios with Au+Au.

We have presented charged hadrons ratios in Fig 6 for the most central collisions. p/π and k/π ratios are presented in Fig 6a, while anti-particle to particle ratios are presented in Fig. 6b. We don't find any configuration dependencies in any of these ratio plots. There is no variation of results observed, when two different systems (Au+Au and U+U) are taken. We guess, although uranium is heavier than gold nucleus as well as more deformed, the similarities in the particle ratios demonstrate their dependencies on the collision energies rather than system sizes. We also find that around $p_T = 1$ GeV, p/π goes higher from k/π ratio. π^-/π^+ remains almost independent of p_T and value of ratio is around unity. However, k^-/k^+ and \bar{p}/p ratios decrease from unity with increasing p_T .

4 Conclusion

We have implemented and tested Nilsson or Modified Harmonic Oscillator(MHO) distribution, to explain some of the observed experimental results for U+U collisions at available RHIC energy within HIJING code. Along with this study, we have shown results from Wood Saxon and

compared with available experimental data. At the first attempt, MHO gives good estimation to experimental charged particle multiplicity distribution as well as to Wood-Saxon formalisms in central collisions. Without any deformation, MHO also reproduces the plateau region of N_{ch} distribution approximately for gold (Au) nuclei collisions, assumed to be spherically symmetric in our present calculations.

In this study we have taken random angle orientation of U nuclei along beam axis as well as two specific orientations, i.e. body-body and tip-tip. Our study shows that within HIJING formalism, tip-tip orientations of colliding nuclei can generate significantly larger number of particles than body-body or orientation average configurations. We observe that body-body configuration gives similar magnitude with that of orientation average.

References

- [1] J. W. Cronin, H. J. Frisch, M. J. Shochet, J. P. Boymond, P. A. Piroue, and R. L. Sumner, Phys. Rev. **D 11**, 3105 (1975)
- [2] K.J. Eskola, V.J. Kolhinen, C.A. Salgado, Eur. Phys. J. **C 9**, 61 (1999)
- [3] Roger D. Woods and David S. Saxon, Phys. Rev. **95**, 577 (1954)
- [4] D.L. Hendrie, N.K. Glendenning, B.G. Harvey, O.N. Jarvis, H.H. Duhm, J. Saudinos, J. Mahoney, Phys. Lett. **B 26**, Issue 3, 127 (1968)
- [5] Hiroshi Masui, Bedangadas Mohanty and Nu Xu; Physics Letters B 679 (2009) 440-444
- [6] Md. Rihan Haque, Zi-Wei Lin and Bedangadas Mohanty, Phys. Rev C **85**, 034905 (2012)
- [7] Pingal Dasgupta, Rupa Chatterjee and Dinesh K. Srivastava Phys. Rev C **95**, 064907 (2017)
- [8] O.S.K. Chaturvedi et. al. Eur. Phys. J. Plus (2017) 132: 430
- [9] Arpit Singh et al, arXiv:1707.07552 [nucl-th]
- [10] S K Tripathy et al, arXiv:1805.02713 [nucl-th]
- [11] Shapes and Shells in nuclear structure, Nilsson and Ragnarsson, Cambridge Univ. Press, 1995
- [12] Structure Of The Nucleus by M. A. Preston, Bhaduri, R. K. Bhaduri, WestView Press (1993)
- [13] Miklos Gyulassy and Xin-Nian Wang, Comput. Phys. Commun. **83** (1994) 307; <http://ntc0.lbl.gov/~xnwang/hijing/>
- [14] Beat Hahn, D. G. Ravenhall, and Robert Hofstadter, Phys. Rev. **101**, 1131 (1956)
- [15] Jerome H. Fregeau and Robert Hofstadter, Phys. Rev. **99**, 1503 (1955)
- [16] B. K. Jennings, R. K. Bhaduri, and M. Brack, Nucl. Phys. **A 253**, 29 (1975)
- [17] J. Dudek, W. Nazarewicz, and P. Olanders, Nucl. Phys. **A420**, 285 (1984)
- [18] R. Bengtsson et al., Physica Scripta **39**, 196 (1989).
- [19] Bao-An Li, Phys. Rev. **C 61**, 021903 (R) (2000)
- [20] P. Moller, J.R. Nix, W.D. Myers and W.J. Swiatecki, Atomic Data and Nuclear Data Tables **59**, 185 (1995)

- [21] L. Adamczyk et al (STAR Collaboration) Phys. Rev. **C 96**, 024905 (2017)
- [22] Hui Wang (Brookhaven National Lab) Quark Matter 2014 - Talk
- [23] A. Adare et al., Phys. Rev. **C 93**, 024901 (2016)